COLOSSAL MAGNETORESISTANCE IN MANGANESE PEROVSKITE FILMS AND MULTILAYERS

I. PANAGIOTOPOULOS, M. PISSAS, C. CHRISTIDES,
G. KALLIAS, V. PSYCHARIS, N. MOUTIS AND D. NIARCHOS
Institute of Materials Science, NCSR Demokritos
Ag. Paraskevi Attikis, 15310 GREECE

1. Introduction

The study of the magnetic properties of mixed valence manganese perovskites dates back almost 50 years [1-2]. The existence of competitive ferromagnetic (FM) double-exchange [3] and antiferromagnetic (AF) superexchange interactions, which are very sensitive to the structural parameters and the degree of doping, results in a very rich magnetic phase diagram for this type of materials [4]. In the case $La_{1-X}Ca_XMnO_3$ of special interest are samples with x~1/3 which show a transition from a low-temperature metallic FM phase to a high temperature semiconducting paramagnetic phase, associated with a very large negative magnetoresistance (MR) effect termed colossal magnetoresistance (CMR). A large number of studies has focused on the interrelated structural, magnetic and MR properties of this type of materials [5-18] as well as the physics of the transition [19-27] in the effort to understand the CMR mechanism and to optimize the materials. However the possibility to use of these materials in technological applications is limited by the large fields (of the order of Tesla) required for saturation. In order to deal with this problem different approaches have been tried [28-31].

Pulsed laser deposition (PLD) has been widely used for the preparation of mixed valence perovskite manganites since the observation of CMR in thin film samples [32,33]. In thin film materials, strain imposed by the substrate, oxygen deficiency and chemical disorder incorporated in the film during deposition can drastically change the CMR properties [32-38]. Thin film samples prepared from stoihiometric $La_{2/3}Ca_{1/3}MnO_{3-\delta}$ targets exhibit a large variety of T_C and resistivity values depending on the preparation conditions [32]. The fact that the T_C and resistivity of these films can be changed by annealing in oxygen atmosphere indicates that the main factor influencing their properties could be some oxygen deficiency, lattice strain and disorder incorporated in the as deposited films. An indication of the latter is the reported small increase of the T_C upon annealing in N_2 atmosphere [39]. Even in polycrystalline $La_{0.67}Ba_{0.33}MnO_{3-\delta}$ samples the transition temperature was reported to shift to lower temperatures and resistivity is to increase with increasing δ [40]. At severely oxygen deficient samples (δ=0.2) the characteristic peak in the ρ *vs* T curve disappears. Since usually greater MR effect is achieved in samples with lower transition temperatures [32,41] $La_{2/3}Ca_{1/3}MnO_{3-\delta}$ films with very negative MR values can be prepared through

I. Nedkov and M. Ausloos (eds.), Nano-Crystalline and Thin Film Magnetic Oxides, 119–132.

proper control of the deposition and annealing conditions. A very high MR value of 127000% has been achieved in $La_{2/3}Ca_{1/3}MnO_3$ films with transition temperatures as low as 77 K compared to the bulk value of 265 K. This extremely large MR effect has been attributed to lattice strain imposed by the substrate since it has been obtained only in films with thickness around 100 nm [42] and under very specific preparation and heat-treatment conditions.

Preparation of artificial structures consisting of different CMR materials is another route to optimize the CMR behavior and understand the mechanisms involved in this phenomenon. The CMR behavior of such structures is not a mere superposition of the response of the individual layers [43]. This could be attributed to either interlayer interactions or stress effects due to lattice mismatch. In what follows we report on the magnetic structural and MR properties of $La_{2/3}Ca_{1/3}MnO_3$ films prepared under different conditions as well as $La_{2/3}Ca_{1/3}MnO_3$ /$La_{1/3}Ca_{2/3}MnO_3$ multilayers showing exchange biasing effects.

2. Experimental details

The films were deposited on (001) $LaAlO_3$ substrates by PLD from bulk stoichiometric $La_{2/3}Ca_{1/3}MnO_3$ target samples. The targets were prepared by standard solid state reaction from La_2O_3, $CaCO_3$ and MnO_2 powders sintered at 1300^{0}C for 5 days with two intermediate grindings. MR measurements were performed with a four probe method and with the current parallel to the applied magnetic field. Stoichiometry was checked by XRF and EDX analysis on films deposited on silicon substrates, since $LaAlO_3$ substrates would not permit the estimation of the La content of the films. The θ-2θ X-ray diffraction data were obtained with a Siemens D500 diffractometer using CuKα radiation and a secondary graphite monochromator. Pole figures obtained by using the Syntex P21 four cycle diffractometer verify the epitaxial growth of the film on the substrate. The magnetic measurements were performed in a SQUID magnetometer (Quondam Design).

3. PLD of $La_{2/3}Ca_{1/3}MnO_{3-\delta}$ films

Due to the structural similarity between manganese perovskites and YBCO superconducting materials much of the previous experience on the PLD deposition of the latter applies also to the former [44]. However in the case of $La_{2/3}Ca_{1/3}MnO_3$ optimum CMR is not observed in fully oxygenated materials so it is meaningful to explore a large variety preparation conditions that differ from those that would yield a perfectly crystallized and oxygenated film material. In our setup the beam of an LPX105 eximer laser (Lambda Physic) with KrF gas (λ=248 nm) was focused on to the target which was rotated during the deposition to minimize target modification effects. The pulse energy is typically 225mJ resulting in a fluence on the target of 1-4 J/cm^2 depending on the spot size. Most of the films considered in this study were prepared at a fluence of 1.5 J/cm^2 and a repetition rate of 6Hz. The substrate temperature (Ts) was varied between 550 and 700^{0}C. The target to substrate distance (d_{TS}) was varied between 2 and 8 cm. The deposition was done in an oxygen atmosphere, the pressure of oxygen was varied between P_{O2}=0.02 and 0.8 Torr.

4. X-ray diffraction

The structure of the target material is orthorhombic and can be described by the space group Pnma. The unit cell constants are a=5.456Å, c=5.451 Å and b=7.747 Å. These parameters are related to the unit cell a_p of the corresponding simple cubic perovskite structure as $a \approx c \approx \sqrt{2}a_p$, $b \approx 2a_p$ which gives a value of $a_p \approx 3.86$ Å. In the X-ray diffraction patterns of the film samples only reflections that can be indexed as 00ℓ of a simple pseudo-cubic perovskite structure appear, indicating a high degree of orientation (Fig. 1). The regions around the (001) and (002) reflections are magnified in the insets. The unit cell constant can be made close to that of the target material (3.86 Å) for a large

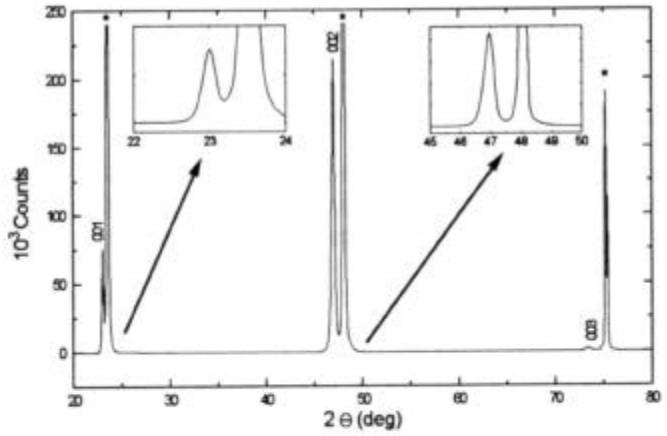

Figure 1. Typical X-ray diffraction pattern of a thin film sample. The regions around the (001) and (002) reflections are magnified in the insets. Reflections due to the $LaAlO_3$ substrate are marked with (*).

variety of preparation conditions. The epitaxy of the films is verified by χ-φ scans performed on the family of [011] reflections with the use of the four cycle diffractometer. Intensity is observed only for four values of φ differing by 90^0 multiples. The values of the φ angles for which the family of the film [011] reflections are observed coincide with those of the substrate [011] reflections.

5. Effect of the deposition conditions

It was observed that irrespectively of the P_{O2} , T_C is higher for films grown at longer distances, that correspond to the visible extent of the plume. This is consistent with the observation that the plasma chemistry is more favorable to proper oxidation when the substrate is located near the edge of the plume. Furthermore, the decreased growth rate, at longer distances, allows more time for crystallization to occur, thus minimizing any disorder. In the films deposited at shorter d_{TS} an increased width of the resistivity peak is observed which is a sign of poor film uniformity. The films deposited at 0.3 Torr and at short distances from the target (2-4 cm) were found to be Mn deficient. This could be

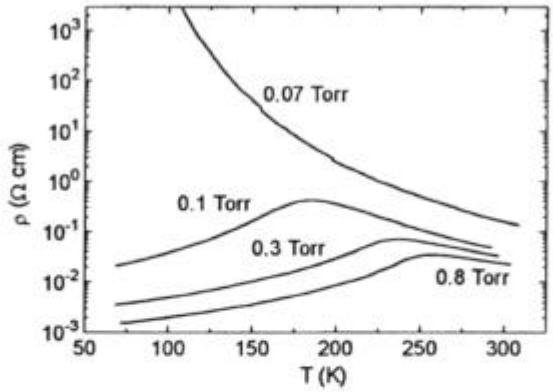

Figure 2. Resistivity as a function of temperature for a series of LaCaMnO thin films prepared under different pressures of oxygen at T_S=700°C and d_{TS}=6 cm.

attributed to secondary ablation on the substrate [44]. The films grown at longer distances have compositions close to the target material. In the case of the films deposited at 0.8 Torr, no significant changes in stoichiometry were observed in the range 2-6 cm.

The properties of the resulting film can be drastically varied by adjusting the preparation conditions. In Fig.2 ρ *vs* T curves are shown for a series of samples prepared under different pressures of oxygen which are noted. The films were prepared at T_S=700°C, d_{TS}=6 cm. Films prepared at higher oxygen pressures have transition temperatures close to that of the bulk material. At lower pressures, higher resistivities and lower transition temperatures are obtained. In films prepared at sufficiently low oxygen pressures the characteristic peak in the ρ *vs* T curve is not observed but instead the samples show an insulating behavior in all the temperature range measured. This happens in a very narrow window of preparation conditions as oxygen pressure is reduced from 0.1 to 0.07 Torr. The double exchange mechanism is based on the hopping of the mobile e_g electron between neighboring Mn ions. Lattice strain affecting the Mn-O-Mn bond angles, oxygen deficiency and disorder are expected to influence this mechanism. Samples prepared under low oxygen pressure or low substrate temperatures are likely to be oxygen deficient, having disordered structures that favor electron localization thus giving rise to lower T_C and increased resistivity. Reduced transition temperatures have also been obtained as T_S was decreased from 700°C to 550°C in films deposited at P_{O2}=0.3 Torr.

6. Films deposited at low P_{O2}

The unit cell constant of the film samples is close to the bulk value of 3.86 Å, despite the large variety of preparation conditions that resulted in very different transition temperatures. However four cycle X-ray diffraction measurements in films deposited in very low oxygen pressures (0.02 Torr, Ts=650°C, d_{TS}=7 cm) reveal a disordered structure with unit cell constants of 3.99 Å perpendicular to the film plane and 3.82 Å parallel to the film plane. This difference between the a and c axis corresponds to an extremely large distortion of the unit cell compared to the ones that can be observed in a

bulk material. The existence of this large distortion is also supported by the fact that the (011) reflection is observed at an angle x ~44^0 with respect to the plane of the substrate instead of the value x=45^0 expected for a perfect cubic crystal (Fig.3). These films show insulating behavior in all the temperature range down to 5 K.

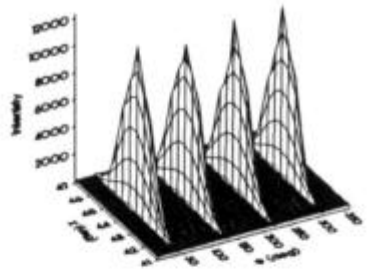

Figure 3. χ-φ scan performed on the family of [011] reflections with the use of a four cycle diffractometer for a film deposited at P=0.02 Torr, TS=650^{0}C and d_{TS}=7 cm .

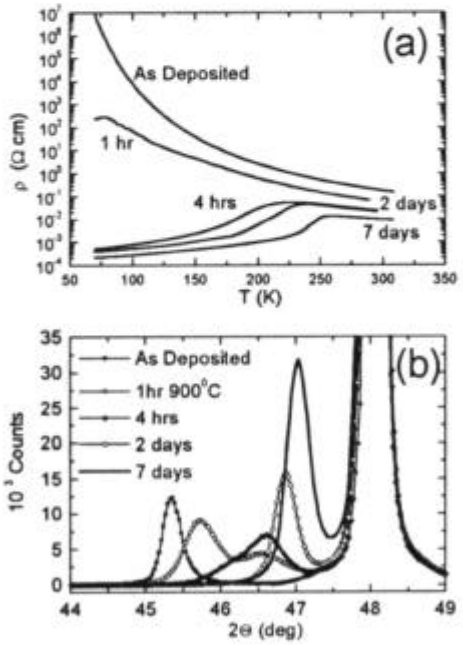

Figure 4. (a) Resistivity as a function of temperature for the as deposited as well as for thin films annealed for different time intervals and (b) the corresponding XRD patterns.

7. Post-annealing of films deposited at low P_{O2}

In Fig.4(a) we present the resistivity as a function of temperature for the as deposited as well as for thin films that were post-annealed for different time intervals. We can see that subsequent heat treatment increases the transition temperature up to values close to that of the target material (265 K). This increase is accompanied by a dramatic decrease of the low temperature resistivity by 6 orders of magnitude. The resistivity at the peak ρ_P decreases as well. Above the T_C an activation law $\rho(T) \propto \exp(E_a/kT)$ was used to fit the data. The activation energy E_a decreases from 1650 K for the as-deposited sample to 710 K for the fully annealed one. The corresponding θ-2θ X-ray diffraction patterns in the region around the (002) peak of the cubic unit cell, which is the strongest peak observed in the θ-2θ plot, are also shown (Fig.4 (b)). The peak is shifted to higher 2θ values finally approaching the value of the bulk material (2θ≈47^0). The films corresponding to 1 hour and 4 hours of annealing are apparently non-homogeneous showing a split peak. XRD measurements on inhomogeneous samples in which the upper part was chemically etched reveal that the lower angle part of the split peak corresponds to the layers closer to the substrate. This is consistent with the fact that these layers are expected to be more strained. The film annealed for 2 days is homogeneous but the peak is

shifted to higher angles after 7 days of annealing. The corresponding displacements are also observed in the (001) and (003) peaks (not shown in the figure).

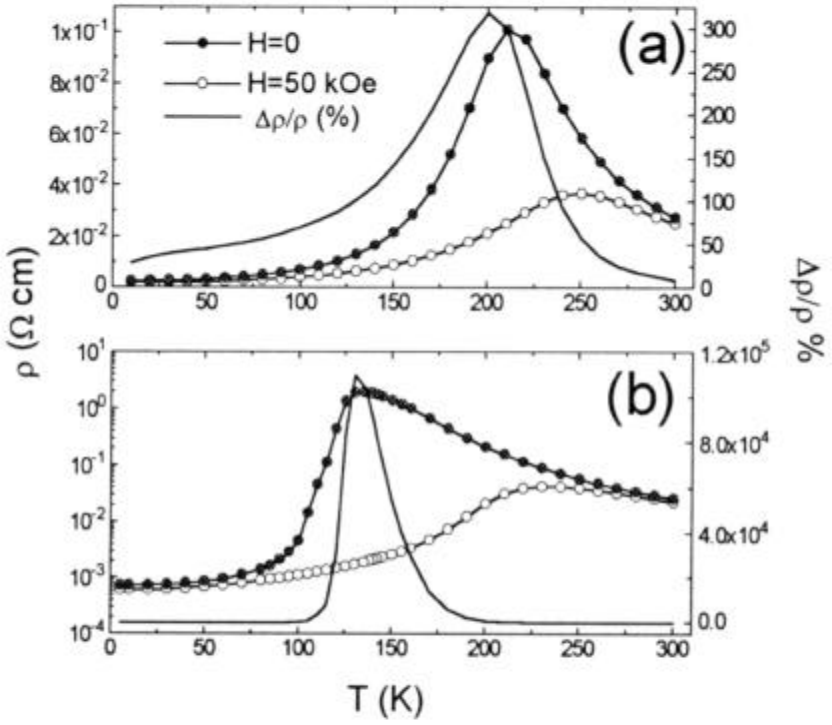

Figure 5. Resistivity as a function of temperature measured in a 50 kOe applied field (○), in zero applied field (●) and magnetoresistance ratio [ρ(0)-ρ(H)]/ρ(H) (—) for samples prepared under different conditions (see text).

8. CMR in $La_{2/3}Ca_{1/3}MnO_{3-\delta}$ films

Fig. 5(a) presents ρ *vs* T measurements in an applied field of 50 kOe as well in zero applied field for a film deposited with oxygen pressure P_{O2}=0.2 Torr and at T_S=700^{0}C. The peak in the resistivity curve is shifted from 210 to 250 K after the application of the magnetic field. The difference between the two curves gives a measure of the MR effect which is plotted as a solid line presenting the ratio [ρ(0)-ρ(H)]/ρ(H). For this film an MR ratio of 320% is obtained at a temperature of 200 K.

It is well established that the size of the CMR effect decreases with increasing T_C and that the highest MR values are observed in films with T_C =77-150 K [32,41]. Thus in order to achieve high MR it seems that the deposition and annealing conditions must be

fine tuned in the low T_C region just before the fully insulating behavior appears. We were able to achieve very high MR ratio values are observed in a film prepared at T_S=700^{0}C, a d_{TS}=6 cm and P_{O2}=0.07 Torr and subsequently annealed at 900^{0}C for 2 days. The peak in the resistivity curve is shifted from 135 to 230 K after the application of the magnetic field and a maximum magnetoresistance of 109000% is obtained at 130 K (Fig. 5(b)). Samples prepared under the same conditions and annealed for times shorter than one day had an insulating behavior in all the temperature range whereas in films annealed for times longer than 3 days the MR effect is substantially decreased. These samples (prepared at T_S=700^{0}C, a d_{TS}=6 cm and P_{O2}=0.07 Torr) are found more difficult to oxidize than the corresponding ones of Fig.5 though deposited at more favorable conditions. The curves 5(a,b) are characteristic of epitaxially grown thin films where grain boundary scattering is not significant [45]. Large MR is observed only around the transition temperature and goes to zero at lower temperatures.

9. Exchange biasing

The existence of unidirectional anisotropy due to exchange coupling between a ferromagnetic (FM) and an antiferromagnetic (AF) phase was discovered by Meiklejohn and Bean [46]. Exchange anisotropy results in a displaced hysteresis loop when the sample is field cooled through the Neél temperature of the AF phase. The microscopic mechanism of loop displacement was originally explained by assuming an ideal AF/FM interface with uncompensated AF moments [46]. The preparation of layered FM/AF structures by modern deposition techniques [47-51] facilitated the efforts to understand the mechanism of exchange biasing and enabled important technological applications as the magnetoresitive spin valve [52]. Up to now exchange anisotropy effects have been studied in mainly in FM/AF systems consisting of transition metal alloys and oxides (e.g. FM=NiFe, Fe_3O_4, and AF=CoO,FeMn). In this work we the study exchange biasing, coercivity and magneto-resistance in a series of $La_{2/3}Ca_{1/3}MnO_3/La_{1/3}Ca_{2/3}MnO_3$ multilayers where the $La_{2/3}Ca_{1/3}MnO_3$ layers are FM and $La_{2/3}Ca_{1/3}MnO_3$ layers are AF. Exchange biasing effects are reported for the first time in a system with this type of magnetic interactions.

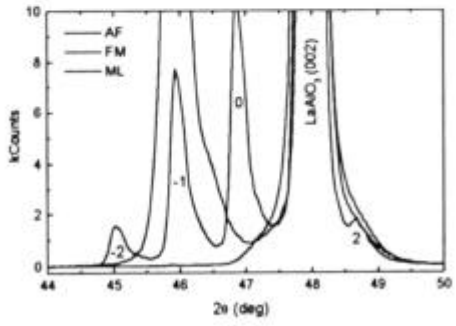

Figure 6. The XRD pattern of a multilayer sample compared to those of single AF and FM layers.

10. PLD of $La_{2/3}Ca_{1/3}MnO_3/La_{1/3}Ca_{2/3}MnO_3$ multilayers

A series of $La_{2/3}Ca_{1/3}MnO_3/La_{1/3}Ca_{2/3}MnO_3$ multilayers with equal AF and FM layer thickness and bilayer thickness ranging from 2 to 32 nm were grown along the (001) direction of the simple pseudocubic perovskite unit cell. The structural compatibility of the AF and FM layers permits coherent growth that favors magnetic coupling. In order to deposit in a multilayer form, the targets were mounted on a step-motor controlled rotatable carrier that allows the $La_{2/3}Ca_{1/3}MnO_3$ and $La_{1/3}Ca_{2/3}MnO_3$ targets to be sequentially exposed in the beam path. The substrate was located at a distance of 6 cm from the target, by the edge of the visible extent of the plume. The substrate temperature (T_s) was 700^{0}C and the oxygen pressure in the chamber during the deposition was 0.03 Torr. The resulting rate at fluence of 1.5 J/cm^2 on the target was 0.4 Å/pulse. The main Bragg peak lies between the Bragg peaks of the single AF and FM layers and is surrounded by satellite peaks due to the layered structure (Fig.6). The existence of an average Bragg peak for $\Lambda \leq 10$nm indicates that for this range of bilayer thickness we have a coherent layer growth. The values of Λ were estimated by the formula $\Lambda = n\lambda_{Cu}/2(\sin\theta_n - \sin\theta_0)$ where θ_n are diffraction angles of the n-th order satellite and θ_0 is the average Bragg peak.

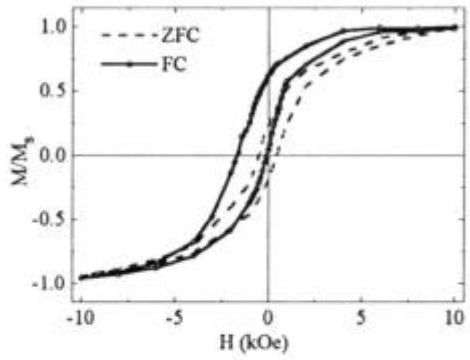

Figure.7 Hysteresis loops, measured at 10 K after cooling down from 300 K in zero field (ZFC) and in 10 kOe (FC), for a

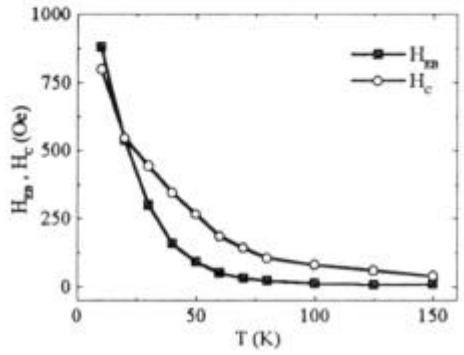

Figure 8. Temperature dependence of exchnage iasing field (H_{EB}) and coercive field (H_C) for the $LaAlO_3/[FM(5\ nm)/AF(5\ nm)]_{15}$ multilayer.

11. Loop Shift

Magnetic hysteresis loops, measured at 10 K after cooling down from 300 K in zero field (ZFC) and in 10 kOe (FC), for a $LaAlO_3/[FM(5\ nm)/AF(5\ nm)]_{15}$ sample are shown in Fig.7. It is evident that the ZFC loop is symmetric around the zero field, while the FC loop is shifted towards negative fields. This effect can be attributed to exchange biasing at the AF/FM

interface, since single-layered FM films do not exhibit any loop displacement after the FC process. If H_1 is the lower and H_2 is the higher field value where the average film magnetization becomes zero, then the exchange biasing field is defined as the loop shift $H_{EB}= -(H_1+H_2)/2$ and the coercivity as the halfwidth of the loop $H_C=(H_1-H_2)/2$. Thus, we calculate for the FC loop an H_{EB}=880 Oe and a H_C=800 Oe which is almost double compared to the H_C value obtained from the ZFC loop. Additional magnetic measurements were performed in order to investigate the origin of this effect. The temperature dependence of H_{EB} and H_C values is shown in Fig.8. These values were estimated from isothermal loops measured in constant temperature intervals, after FC the sample from 300 K down to 10 K in 10 kOe and then warming up. It is evident that H_{EB} decreases and disappears around the so-called blocking temperature T_B of 70 K. The H_C values exhibit a similar trend, indicating a connection between the mechanisms that give rise to coercivity and loop displacement.

In Fig.9 the ZFC(W)and FC(W) measurements of the average film magnetization as a function of temperature are shown. Both measurements were performed by warming up in 1 kOe after having cooled in zero field and 10 kOe respectively. The ZFC and FC curves coincide at temperatures higher than 100 K and become zero at about 250 K, where the Curie point T_c of the FM layers is expected. The ZFC curve exhibits a broad peak around the T_B~70 K, whereas the FC curve exhibits a steep increase just below T_B. It is reasonable to assume that the increase of magnetization in the FC measurement results from the alignment of interfacial magnetic moments, giving rise to unidirectional anisotropy below T_B [45]. Hence, the observed hump below T_B in the ZFC curve can be attributed to thermally activated magnetic rotation over energy barriers caused by random exchange coupling at the AF/FM interfaces.

12. Bilayer thickness dependence of exchange biasing phenomena

Since exchange biasing is an interface related phenomenon a strong dependence on the individual FM and AF layer thicknesses is expected. In order to establish such a layer thickness dependence a series of multilayers with equal AF and FM layer thicknesses $LaAlO_3/[FM(\Lambda/2)/AF(\Lambda/2)]_{15}$ has been studied. Remarkably our M vs T measurements indicate that the T_B does not change in the examined range of bilayer thicknesses and occurs around 70 K for all samples (Fig.9). This would mean that the mechanism of the interfacial spin ordering does not depend o the layer thickness.

Fig.10 shows the variation of the normalized resistivity as a function of temperature, measured in 50 kOe (ρ_H) and in zero applied field (ρ_0). Again the solid line represents the $\Delta\rho/\rho_H=[\rho_0-\rho_H]/\rho_H$ ratio that gives an estimate of the CMR effect. The resistivity increases drastically as we cool down from 300 K, spanning several orders of magnitude. This can be attributed to the presence of the insulating AF layers that mask the response of to the FM layers. However we can see that for the samples with maximum exchange biasing effects a peak is observed around T_B that can be attributed to the alignment of the interfacial spins, whereas MR is also maximized around the same temperature range. This is in agreement with the M *vs* T measurements (Fig.9) where it is evident that the most drastic change of the average film magnetization does not occur near the T_c of the individual FM layers but at T_B.

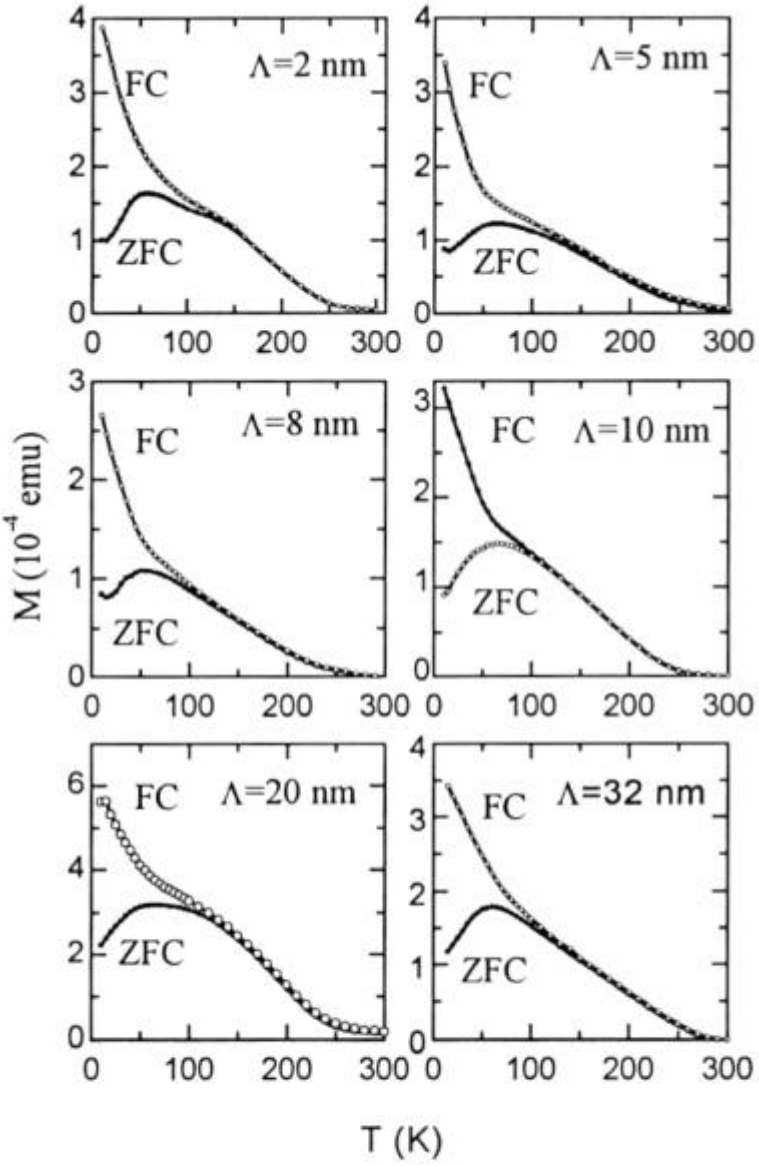

Figure.9 Magnetization as a function of temperature for the series of $[FM(\Lambda/2nm)/AF(\Lambda/2nm)]_{15}$ *multilayers. The measurements were performed by warming up in 1 kOe after having cooled down to 10 K, in zero field (ZFC) and 10 kOe (FC) respectively.*

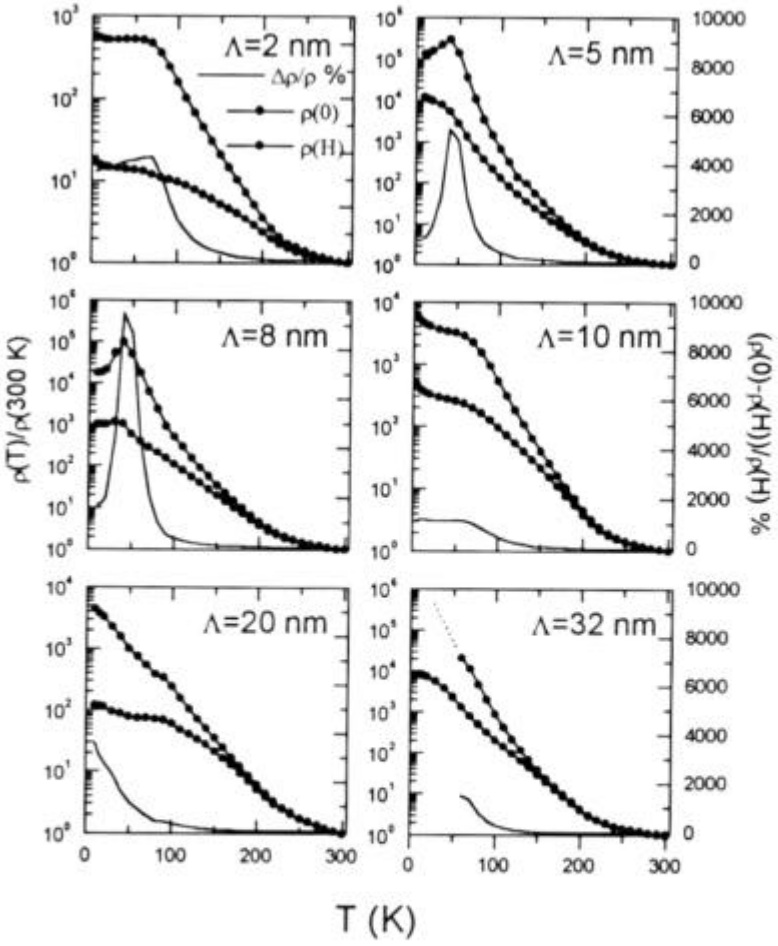

Figure.10 Resistivity, normalized to the 300 K value, as a function of temperature, measured in 50 kOe (ρ_H) and in zero applied field (ρ_0) for the series of $[FM(\Lambda/2)/AF(\Lambda/2)]_{13}$ multilayers. The CMR ratio $\Delta\rho/\rho_H=[\rho_0-\rho_H]/\rho_H$ is plotted as a solid line.

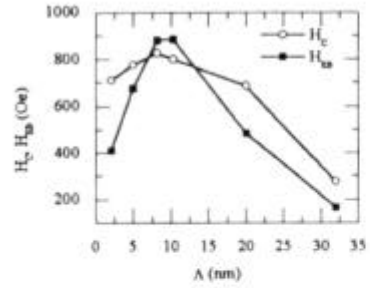

Figure 11. Exchnage biasing field (H_{EB}) and coercive field (H_C) as a function of the bilayer thickness Λ for the series of $LaAlO_3/[FM(\Lambda/2)/AF(\Lambda/2)]_{15}$ multilayers.

The observed H_{EB} and H_C values at 10 K, are plotted in fig.11 as a function of the bilayer thickness Λ. The maximum H_{EB} is observed for the sample with Λ=10 nm. At higher bilayer thicknesses H_{EB} decreases as expected due to decreased role of the interface exchange coupling. A decrease is also observed at lower Λ due to the reduced thickness of the AF layer [51]. Again, the H_C follows the variation of H_{EB} with Λ, indicating that there is a significant contribution in H_c from the exchange anisotropy at the AF/FM interfaces.

13. Conclusions

Films deposited from $La_{2/3}Ca_{1/3}MnO_3$ targets exhibit a large variety of magneto-transport properties depending on the exact preparation conditions and subsequent heat-treatments performed. Films deposited at higher oxygen pressures, at T_S=700^{0}C and at target to substrate distances corresponding to the visible extent of the plume have properties similar to those of the target material. At lower P_{O2} or T_S films with lower T_C and higher resistivity are obtained. When films are prepared under very low (P_{O2}=0.02 Torr) oxygen pressures a distorted structure is obtained, exhibiting insulating behavior in all the temperature range. Upon annealing at 900^{0}C in oxygen flow for several days the bulk properties can be regained and therefore these differences must be attributed to lattice strain and oxygen deficiency in the thin film materials. This annealing probably leads to recrystallization towards a more stable state, reducing in this way stoichiometric gradients as well as oxygen and cation inhomogeneities. A series of $[La_{2/3}Ca_{1/3}MnO_3/La_{1/3}Ca_{2/3}MnO_3]_{15}$ multilayers, with bilayer thicknesses between 2 and 32 nm, has been prepared by Pulsed Laser Deposition. The study of their magnetic and magnetotransport properties reveals, for the first time in this category of materials, the presence of an exchange biasing mechanism at low temperatures. Zero-field-cooling and field-cooling magnetic measurements reveal a blocking temperature around 70 K that is independent from the bilayer thickness, whereas the average film magnetization becomes zero at 250 K.

REFERENCES

1. G.H. Jonker and J.H. Van Santen, Physica (Utrecht)16, 337 (1950)
2. E. O. Wollan and W.C. Koehler Phys. Rev 100, 545-563 (1955)
3. C. Zener, Phys. Rev. **81**, 440 (1951);**82** 403 (1955); P.W. Anderson, H. Hasegawa, Phys. Rev. **100**, 675 (1995)
4. P. Schiffer, A.P. Ramirez, W. Bao, and S-W. Cheong, Phys. Rev. Lett. **75,** 3336 (1995).
5. R. Mahesh, R. Mahendiran, A.K. Raychauduri and C.N.R. Rao, J. Solid. State Chem. **120**, 204 (1995)
6. H.Y. Hwang, S-W. Cheong, P.G. Radaelli, M. Marezio, and B. Batlogg, Phys. Rev. Lett. **75**(5) 914, (1995)
7. J.M.D. Coey, M. Viret, L. Ranno, K. Ounadjela, Phys. Rev. Lett. **75**, 3910 (1995)
8. J. Fontcuberta, B. Martinez, A. Seffar, S. Pinol, J.L. Garcia-Munoz, and X. Obradors, Phys. Rev. Lett. **76**, 1122 (1996)
9. J. Blasco, J. Garcia, J.M. De Teresa, M. R. Ibarra, P.A. Algarabel and, C. Marquina, J. Phys. Condens. Matter **8** (1996) 7427 (1996)
10. Maignan, Ch. Simon, V. Caignaert, B. Raveau Z. Phys. **B 99**, 305 (1996)
11. P.G. Radaelli G. Iannone, M. Marezio, H.Y. Hwang, S-W. Cheong, J.D. Jorgensen and D.N. Argyriou., Phys. Rev. B **56**, 8265 (1997)
12. P.G. Radaelli,M. Marezio, H.Y. Hwang, S-W. Cheong, J. Solid. State Chem.**122**, 444 (1996)
13. H. Kuwahara, Y. Moritomo, Y. Tomioka, A. Asamitsu, M. Kasai, Y. Tokura J. Appl. Phys. **81**(8), 4954 (1997)
14. Y. Tomioka, H. Kuwahara, A. Asamitsu, M. Kasai, Y. Tokura, Appl. Phys. Lett. **70**(26), 3609 (1997)
15. Sundaresan , A Magnain, B.Raveau, Phys. Rev. B **56**, 5092 (1997)
16. F. Millange, A. Maignan, V Caignaert,C Simon, B Raveau, Z. Phys B 101, 169 (1996)
17. M. Medarde J. Mesot, P. Lacorre, S. Rosenkranz, P. Fisher and K. Gobrecht, Phys. Rev. B **52** 9248 (1995)
18. L.M Rodriguez-Martinez and J. P. Attfield, Phys. Rev. B **54**(22) R15662 (1996)
19. A.J. Millis, P.B. Littlewood, and B.I. Shraiman Phys. Rev. Lett. **74**, 5144 (1995);
20. A.J. Millis, B.I. Shraiman and, R. Mueller Phys. Rev. Lett. 77, 175 (1996)
21. H. Röder, Jun Zang and A.R. Bishop, Phys. Rev. Lett. **76**, 1356 (1996)
22. J. J. Neumeier, M. F. Hundley, J. D. Thompson and R. H. Heffner, Phys. Rev. B **52**, R7006 (1995)
23. J.W. Lynn, R.W. Erwin, J.A. Bochers, Q. Huang,A. Santoro, J-L. Peng and Z.Y. Li, Phys. Rev. Lett. **76**, 4046 (1996)
24. R. H. Heffner, L.P. Le, M.F. Hundley, J.J. Neumeier, G.M. Luke, K. Kojima, Nachumi, Y.J. Uemura, D.E. MacLaughlin and S-W. Cheong, Phys. Rev. Lett. **77**, 1869 (1996)
25. J.M. De Teresa, M.R. Ibarra, P.A. Algarabel, C. Ritter, C. Marquina, J. Blasco,J.Garcia, A. del Moral and Z. Arnold, Nature **386**, 256 (1997)
26. J.A. Fernandez-Baca, P. Dai, H.Y. Hwang, C. Kloc and S-W. Cheong, Phys. Rev. Lett. **80**, 4012 (1998)

27. N. Moutis, I. Panagiotopoulos, M. Pissas and D. Niarchos in Phys. Rev B. to be published
28. Yu Lu et. al. Phys. Rev. B **54** R8357 (1996)
29. J. S. Sun et. al Appl. Phys. Lett. **69** 3226 (1996)
30. N.D. Mathur et. al. Nature **387** (1997)
31. H.Y. Hwang et. al. Appl. Phys. Lett. **68** 3494 (1996)
32. S. Jin, T.H. Tiefel, M. Mc Cormack, R. A. Fastnacht,R. Ramesh, L.H. Chen, Science **264**, 413 (1994)
33. R. von Helmot, J. Wecker, B. Holzapfel, L.Shultz and K. Samwer, Phys. Rev. Lett. **71**, 2331 (1993)
34. K.M. Satayalakshmi, S. Sundar Manoharan, M.S. Hedge, V. Prasad and S.V. Subramanyam ; J. Appl. Phys. **78**(11), 6861 (1995)
35. Y.Q. Li, J. Zhang, S. Pombrik, S. DiMascio, W. Stevens, Y.F. Yan and N.P. Ong J. Mater. Res. **10**,2167 (1995)
36. S. Freisem, A. Brockhoff, D.G. de Groot, B. Dam and J. Aarts; J. Magn. Magn. Mat. **165**, 380 (1997)
37. T.Y. Koo, S.H. Park, K.-B. Lee and Y.H. Jeong; Appl. Phys. Lett. **71**, 997 (1997)
38. E.S. Vlakhov, R.A. Chakalov, R.I. Chakalova, K.A. Nenkov, K. Dörr, A. Handstein and K.-H. Müller; J. Appl. Phys. **83**(4), 2152 (1998)
39. H.L. Ju, C. Kwon, Qi Li, R.L. Greene, and T. Venkatesan, Appl. Phys. Lett. **65(16),** 2108 (1994)
40. H.L. Ju, J. Gopalakrishnan, J.L. Peng, Qi Li, G.C. Xiong, T Venkatesan and R.L Greene; Phys. Rev B **51**, 6143 (1995)
41. S. Jin, T.H. Tiefel, M. Mc Cormack, M.O'Bryan, L.H. Chen, R. Ramesh , D. Shurig; Appl. Phys. Lett. **67(4)** 557 (1995)
42. Rongsheng Cheng, Kebin Li, shouguo Wang, Zhixiang Chen, Caoshui Xiong, Xiaojun Xu and Yuheng Zhang, Appl. Phys. Lett. **72**, 2475 (1998)
43. H.F. Sakeek, M Higgins, W.G. Graham, T. Morrow, R.J. Turner, and D.G. Walmsley, J. Appl. Phys. **70(4),** 2455 (1991)
44. M.F. Hundley, J.J. Neumeier, R.H. Heffner, Q.X. Jia, X.D. Wu and J.D. Thompson J. Appl. Phys. **79(8)**, 4535-4536 (1996)
45. A. Gupta, G.Q. Gong, G. Xiao, P.R. Duncoube, P. Lecoeur, P. Trouilloud, Y.Y. Wang and J.Z. Sun Phys. Rev. B. **54,** 15629, (1996)
46. W.H. Meiklejohn and C.P. Bean; Phys. Rev. **105**(3), 904 (1957).
47. C. Tsang and K. Lee; J. Appl.Phys.**52**(3), 2471 (1981).
48. P.J. van der Zaag, A.R. Ball, L.F. Feiner, R.M. Wolf and P.A.A. van er Heijden; J. Appl. Phys. **79**, 5103 (1996).
49. J. Nogues, D. Lederman, T.J.Moran I. Shuller and K.V. Rao; Appl. Phys. Lett. **68**(22),3186 (1998).
50. K. Takano, R.H. Kodama, A.E. Berkowitz, W. Cao G. Thomas, Phys. Rev. Lett. **79**, 1130 (1997).
51. R. Jungblut, R. Coehorn, M.T. Johnson, J. van ce Stegge and A. Reinders, J. Appl. Phys. **75**, 6659, (1994).
52. B. Dieny, V.S. Speriosu, S.S.P. Parkin, B.A. Gurney, D.R. Wilhout, and D. Mauri, Phys. Rev. B **43**, 1297 (1991)